Supplementary Material

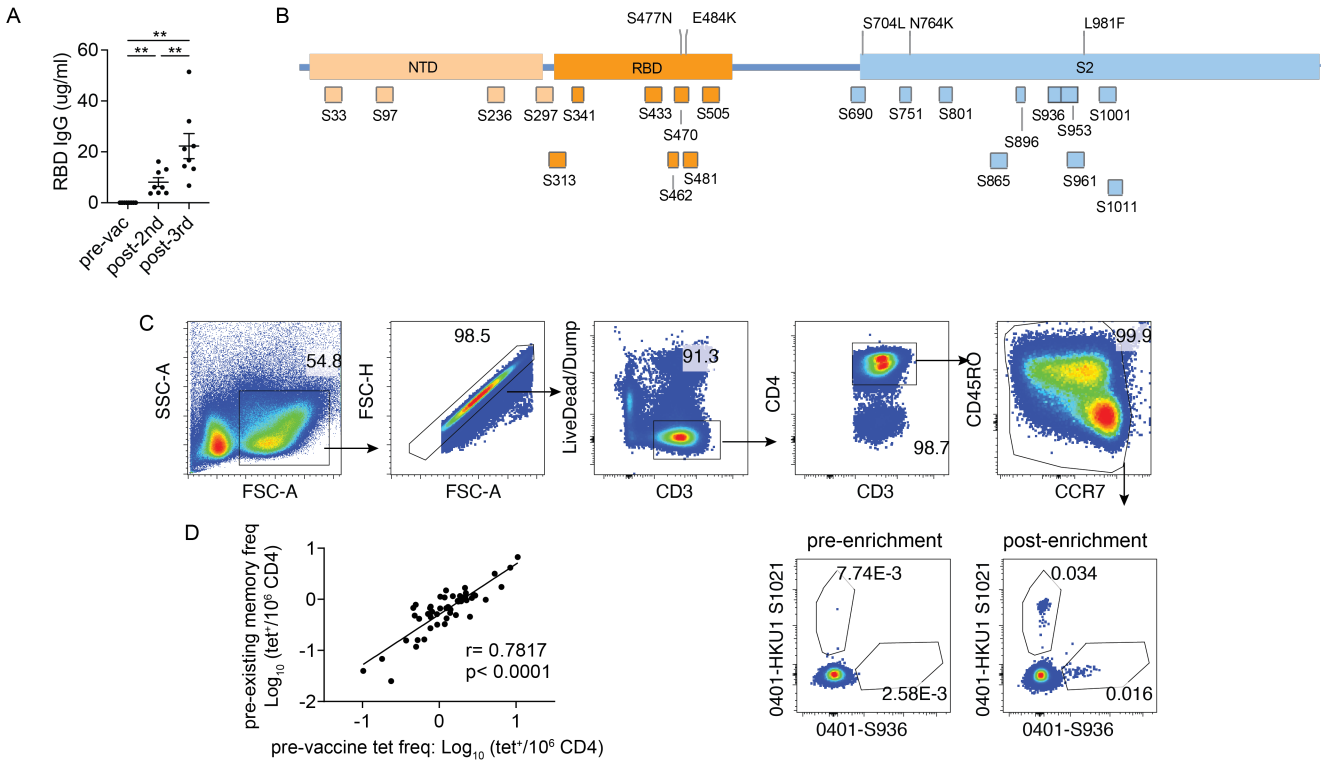


Figure S1: SARS-CoV-2 epitopes and gating strategies. (A) RBD-specific IgG levels measured in plasma collected at the indicated time points. RM one-way ANOVA with Holm-Sidak multiple comparison test was performed. (B) Schematic of spike protein showing the position of peptides used in direct ex vivo tetramer analysis. (C) Representative plots show the gating strategy for identifying tetramer$^+$ cells. (D) Correlation between the frequency of tetramer$^+$ T cell and pre-existing memory T cells within each population in the pre-vaccine samples (n = 50). Association was measured by Spearman correlation. The representative pre- and posts-enrichment plots shown S1C is identical to that presented in Fig. 1B.

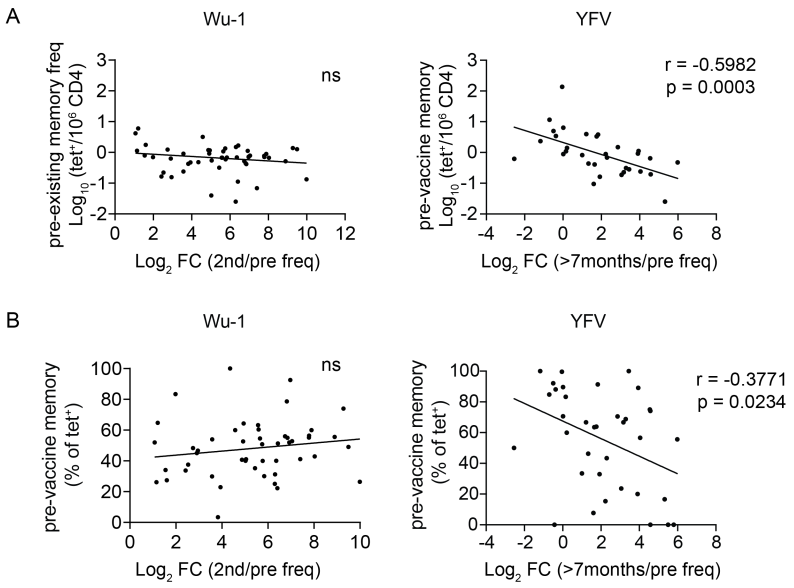


Figure S2: Correlation between baseline memory and YFV or COVID-19 vaccine responses.
(A-B) Relationship between fold change in tetramer$^+$ T cells after two-dose COVID-19 vaccination (left) or YFV vaccination (right) and pre-existing memory in the pre-vaccination samples, measured as frequency (A) or percentage of tetramer$^+$ cells (B). Pearson or Spearman correlation was used depending on normality testing.

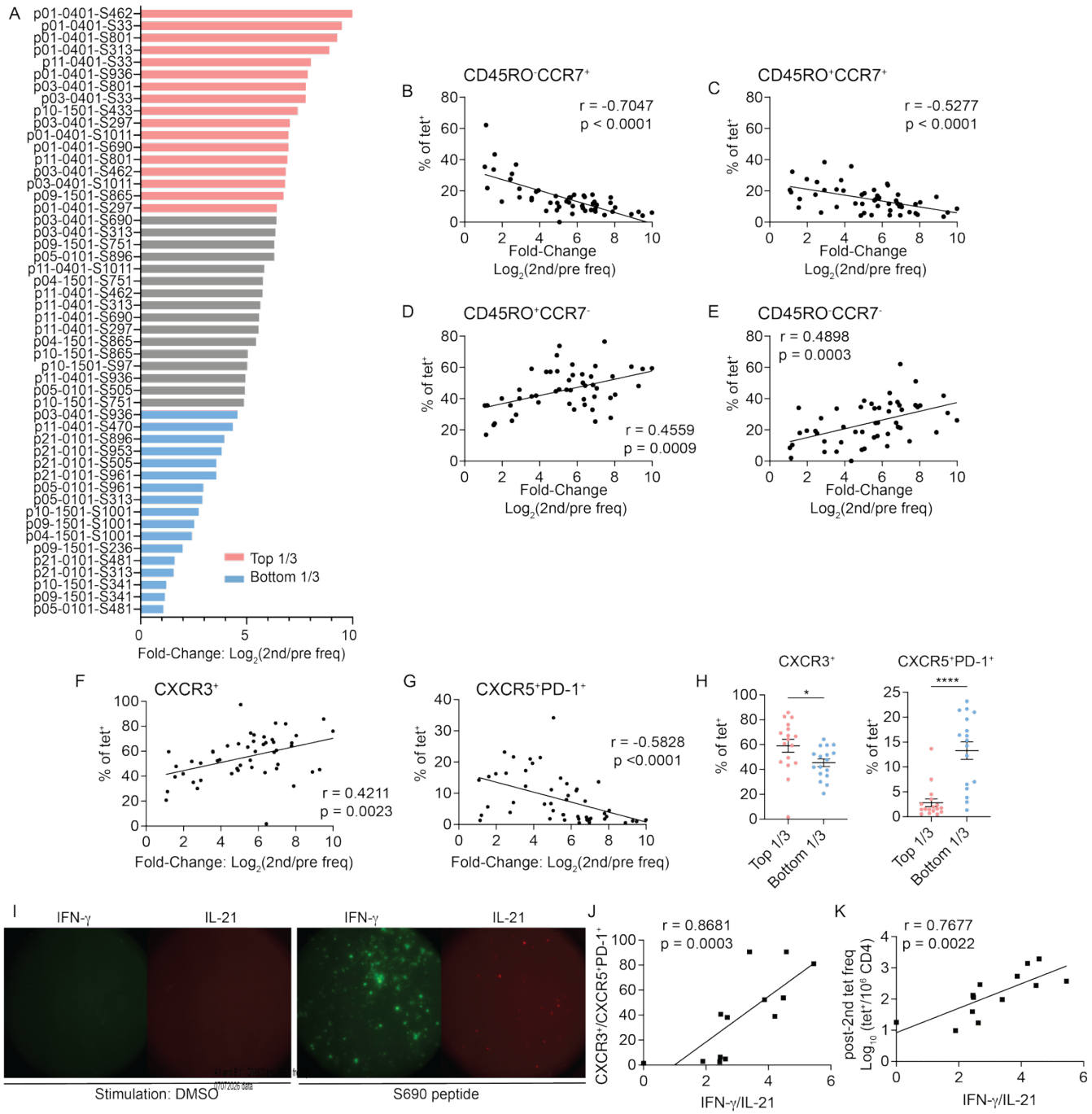


Figure S3: Response to vaccination is associated with distinct functional bias.
(A) Wu-1 tetramer$^+$ CD4$^+$ T cell populations ranked by fold change from baseline after the 2nd dose. Each bar represents a unique vaccine-specific population labeled by participant (p) ID, MHC allele, and spike peptide. (B-E) The relationship between the percentage of naïve-like (B), CM (C), EM (D), and TEMRA (E) subsets within tetramer$^+$ populations and vaccine-induced fold change after the 2nd dose (n = 50). Pearson or Spearman correlation was used depending on normality testing. (F) Correlation between FC from baseline and the proportion of CXCR3$^+$ cells after the 2-dose vaccination. Pearson correlation was used. (G) Correlation between FC and CXCR5$^+$PD-1$^+$ percentage within tetramer$^+$ cells post-vaccination. Spearman correlation was used. (H) Percentage of CXCR3$^+$ and CXCR5$^+$PD-1$^+$ cells in the top and bottom tertile post-2nd dose. Welch's t-test or Mann–Whitney test was used based on normality testing. (I) Representative images show IFN-γ (AF488) and IL-21 (CTL-Red) secreting cells by FluoroSpot under the indicated stimulation conditions. (J) The relationship between IFN- γ/IL-21 and CXCR3$^+$/CXCR5$^+$PD-1$^+$ ratio. Spearman correlation was used. (K)

Correlation between IFN- γ/IL-21 ratio and tetramer$^+$ frequency after the 2nd vaccine dose. Pearson correlation was used.

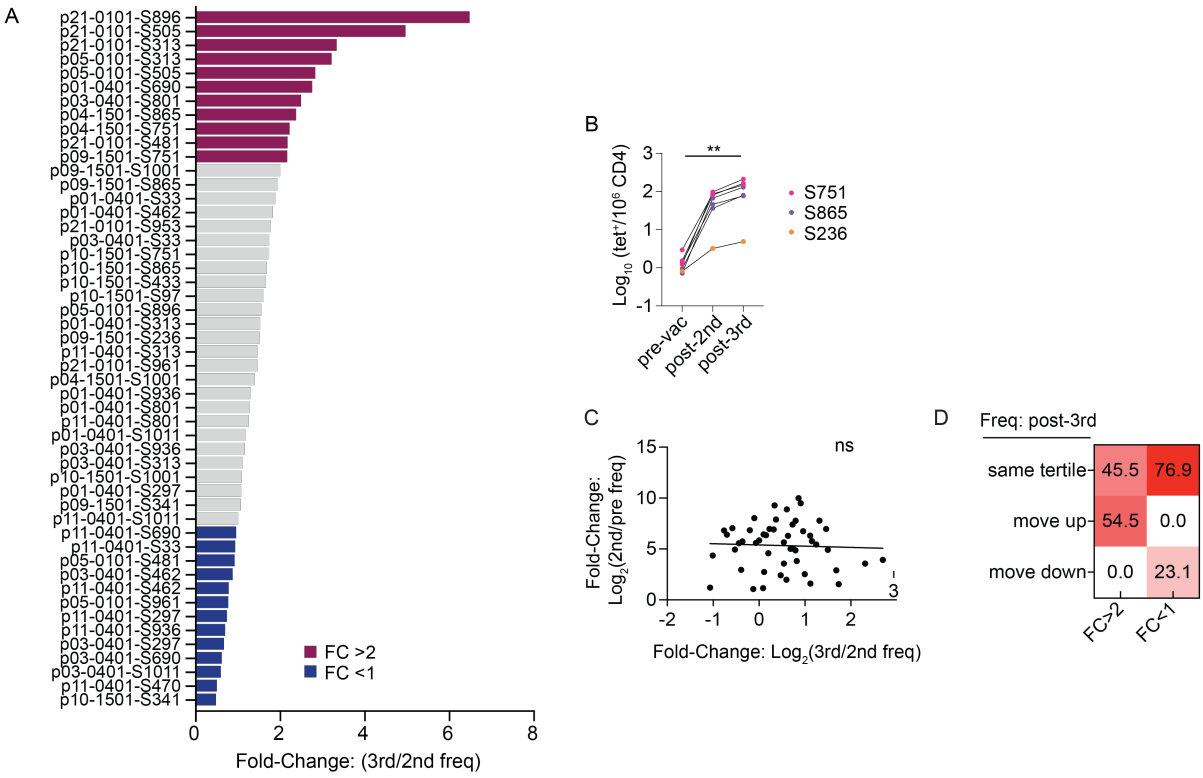


Figure S4: booster vaccination elicits heterogeneous responses.
(A) Distribution of Wu-1 tetramer$^+$ populations ranked by fold change from the post-2nd-dose baseline after the 3rd vaccine dose. Each bar represents a unique vaccine-specific population labeled by participant ID, MHC allele, and spike peptide. Fold changes were calculated as geometric mean. (B) Frequency of S751-, S865-, and S236-specific T cells at the indicated time points, colored by specificity. Friedman test with Dunn's multiple comparisons test was used. (C) Correlation between responses to the initial 2-dose series (post-2nd/pre) and responses to the booster (post-3rd/post-2nd) (n = 50). Pearson correlation was performed. (D) Heatmap summarizes the percentage of FC > 2 (n = 11) or FC < 1 (n = 13) tetramer$^+$ populations that stayed or moved into the higher or lower frequency tier after the third vaccine dose.

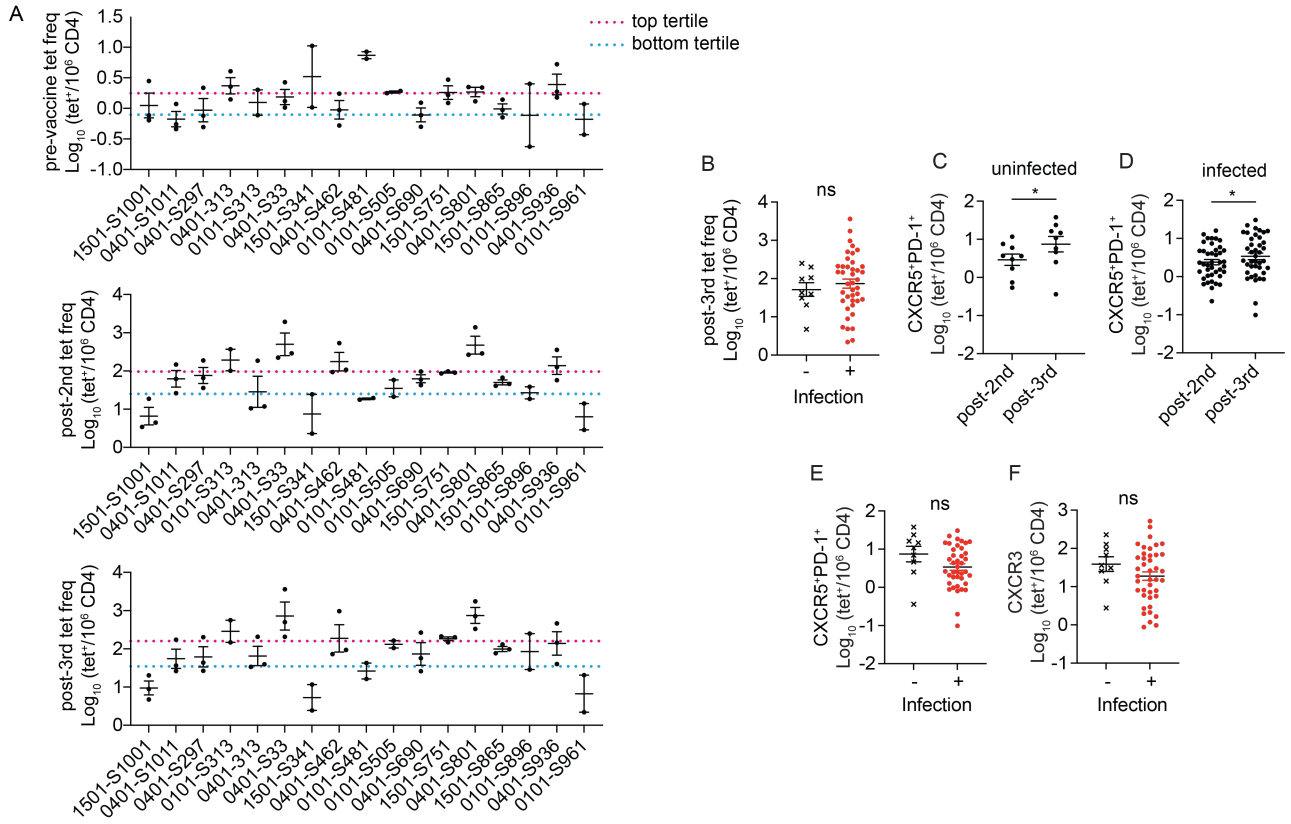


Figure S5: Spike-specific vaccine responses across donors and by COVID-19 infection status.
(A) Plots show tetramer$^+$ populations for epitopes quantified in at least two individuals. Each dot represents a different donor for that specificity. Populations were ranked by frequency and divided into tertiles. Differences in the distribution of populations across tertiles of responses were assessed using the Fisher's Exact test: not significant pre-vaccination, $p < 0.001$ post-2nd dose, $p = 0.009$ post-3rd dose. (B) Frequencies of Wu-1 tetramer$^+$ populations after the booster, stratified by participant infection status between the 2nd and 3rd vaccine doses (uninfected, n = 9; infected, n = 41). Welch's t-test was performed. (C-D) Frequencies of CXCR5$^+$PD-1$^+$ tetramer$^+$ cells after the 2nd and 3rd vaccine doses from uninfected participants (C) or individuals with COVID-19 infection between doses 2 and 3 (D). Paired t-test was used. (E-F) Frequencies of tetramer$^+$ cells expressing Tfh (E) or Th1 phenotype (F), stratified by infection status. Welch's t-test was used.

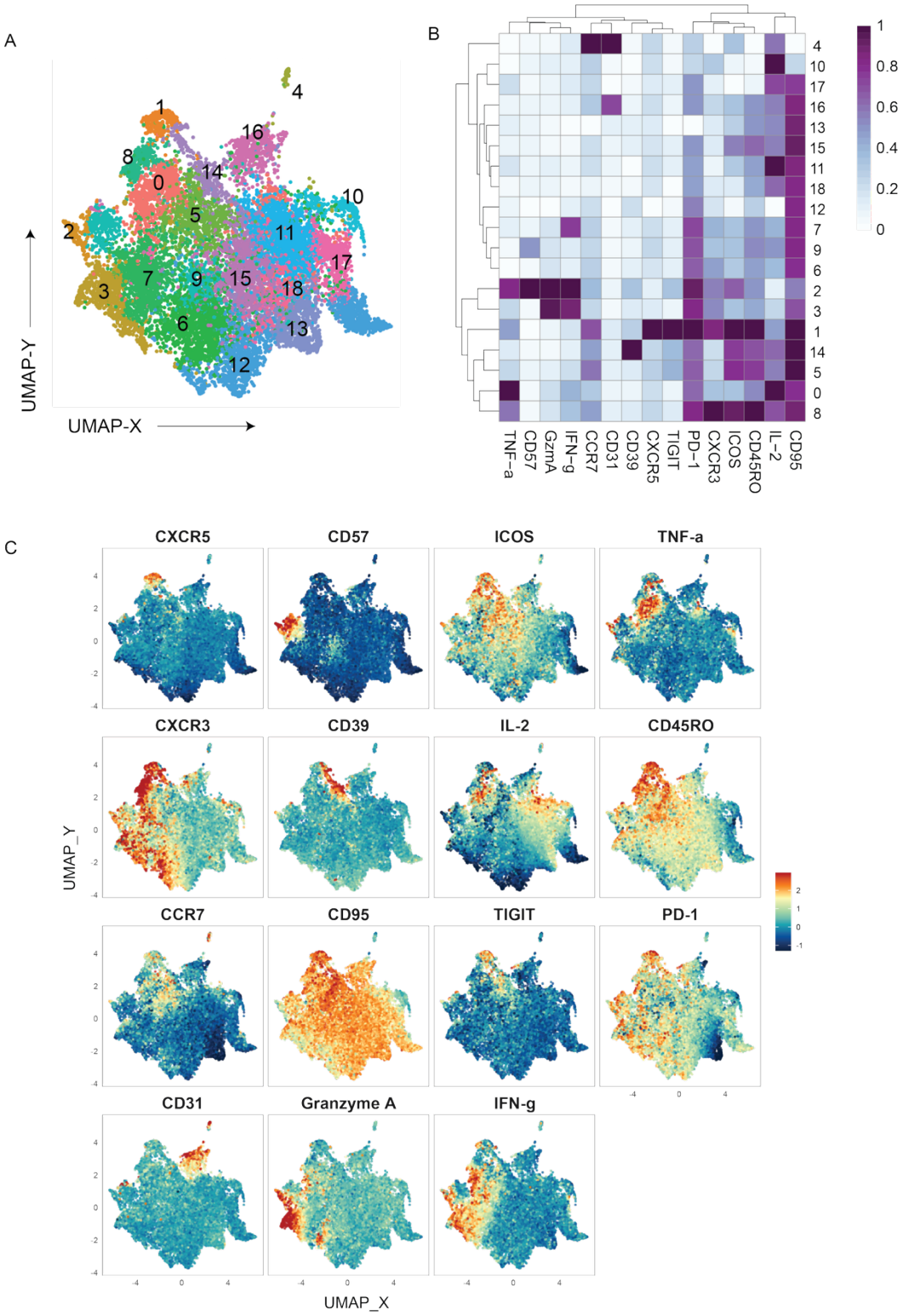


Figure S6: Phenotypic landscape of SARS-CoV-2–specific CD4⁺ T cells after booster.
(A) UMAP displays phenograph-defined clusters of Wu-1–specific CD4⁺ T cells. (B) Heatmap shows the median staining signal of individual markers for clusters shown in (A). (C) UMAPs display the staining intensity of the indicated markers. Data include 15,432 cells from 24 tetramer⁺ populations in post–3rd dose blood samples from 7 individuals.

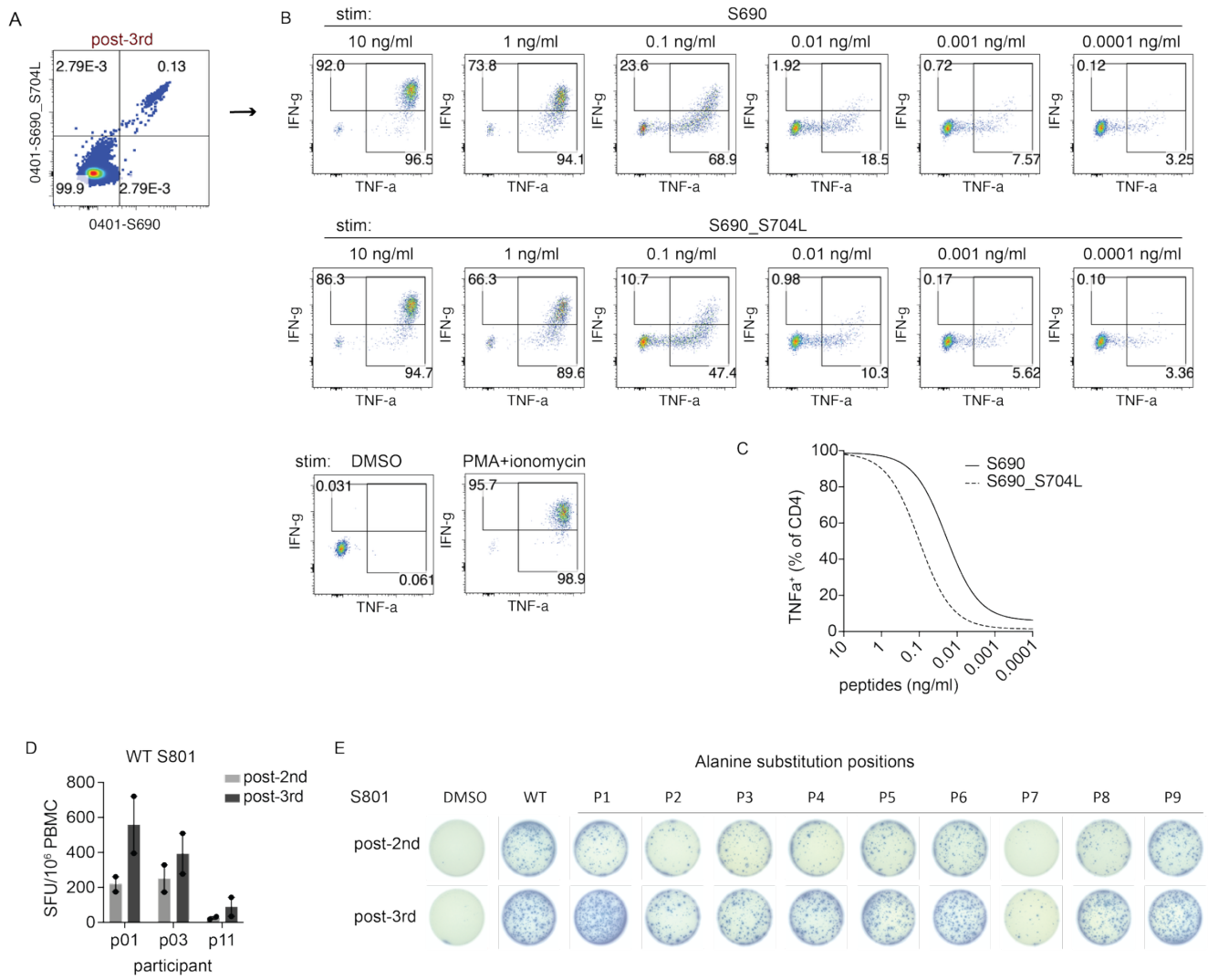


Figure S7: Cross-recognition of variant sequences by Wu-1 tetramer$^+$ CD4$^+$ T cells.
(A) S690$^+$S690_S704L tetramer$^+$ cells from a post-3rd COVID-19 vaccine sample were sorted to generate single-cell clones. FACS plot of ex vivo tetramer staining. (B) Single-cell derived T cell clones were co-cultured for 5-hours with monocyte-derived DCs treated with DMSO vehicle control, PMA and ionomycin, or decreasing concentrations of S690 or S690_S704L peptides. Plots show representative cytokine response for the indicated conditions. (C) TNF-α dose response curve following stimulation with S690 or S690_S704L peptides from a reprentative clone. (D) Frequency of IFN-γ–secreting cells following 48 hours of WT S801 stimulation in PBMCs from three participants after the 2nd or 3rd vaccine dose. (E) Representative ELISpot images showing IFN-γ–secreting cells after stimulation with DMSO, WT S801 sequence, or alanine-substituted S801 peptides using samples collected after the 2nd and 3rd vaccine doses.

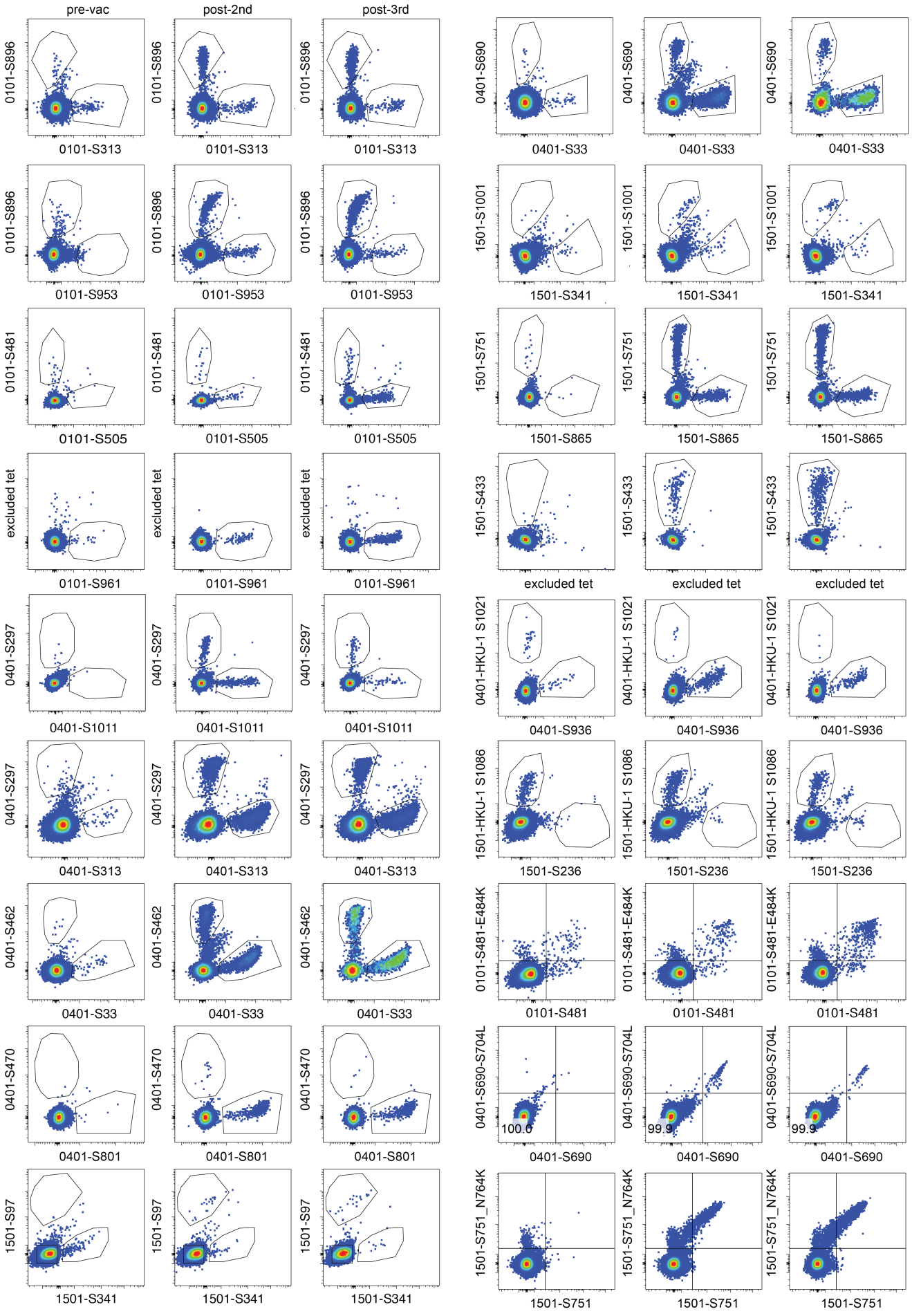

pre-vac
post-2nd
post-3rd
0101-S896
0101-S313
0101-S953
0101-S481
0101-S505
excluded tet
0101-S961
0401-S297
0401-S1011
0401-S313
0401-S462
0401-S33
0401-S470
0401-S801
1501-S97
1501-S341
0401-S690
0401-S33
1501-S1001
1501-S341
1501-S751
1501-S865
1501-S433
excluded tet
0401-HKU-1 S1021
0401-S936
1501-HKU-1 S1086
1501-S236
0101-S481-E484K
0101-S481
0401-S690-S704L
0401-S690
100.0
99.9
99.9
1501-S751_N764K
1501-S751

Figure S8: Tetramer-labeled spike-specific CD4^{+} T cells.
Representative flow plots of individual specificities detected by pMHC tetramers. PBMCs collected before vaccination and after the second and the third vaccine doses were analyzed in the same experiment. Plots show tetramer staining in the elute fraction following magnetic column enrichment and include ones identical to that presented in Fig. 2A and 3D.

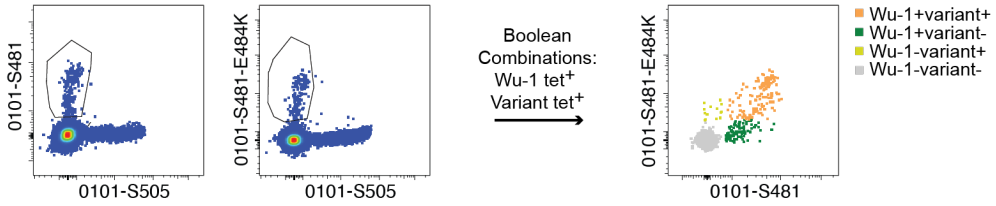


Figure S9: Gating strategy used to identify Wu-1-only, variant-only, and cross-reactive T cell populations. Wu-1- and variant-tetramer-positive cells were gated against another spike specificity and classified by Boolean gating as Wu-1-only, variant-only, or dual-positive.